Hindawi Publishing Corporation
Advances in Condensed Matter Physics
Volume 2015, Article ID 403196, 8 pages
http://dx.doi.org/10.1155/2015/403196

Research Article

Optical Properties of Sol-Gel Nb_2O_5 Films with Tunable Porosity for Sensing Applications

Rosen Georgiev, Biliana Georgieva, Marina Vasileva, Petar Ivanov, and Tsvetanka Babeva

Institute of Optical Materials and Technologies "Acad. J. Malinowski", Bulgarian Academy of Sciences, Acad. G. Bonchev Street, Block 109, 1113 Sofia, Bulgaria

Correspondence should be addressed to Tsvetanka Babeva; babeva@iomt.bas.bg

Received 10 May 2015; Accepted 16 June 2015

Academic Editor: Rosa Lukaszew

Thin Nb_2O_5 films with tunable porosity are deposited by the sol-gel and evaporation induced self-assembly methods using organic template Pluronic PE6100 with different molar fractions with respect to $NbCl_5$ used as a precursor for synthesis of Nb sol. Surface morphology and structure of the films are studied by Transmission Electron Microscopy and Selected Area Electron Diffraction. The optical characterization of the films is carried out through reflectance spectra measurements of the films deposited on silicon substrates and theoretical modeling in order to obtain refractive index, extinction coefficient, and thickness of the films. The overall porosity of the films and the amount of adsorbed acetone vapors in the pores are quantified by means of Bruggeman effective medium approximation using already determined optical constants. The sensing properties of the samples are studied by measuring both the reflectance spectra and room-temperature photoluminescence spectra prior to and after exposure to acetone vapors and liquid, respectively. The potential of using the studied mesoporous Nb_2O_5 films for chemooptical sensing is demonstrated and discussed.

1. Introduction

In recent years, Nb_2O_5 emerges as a multifunctional material due to its interesting properties such as electrochromic behavior [1], photoelectric and photocatalytic activity [2], excellent chemical stability, and corrosion resistance in both acidic and alkaline media [3]. Besides, many applications in photonics demand high refractive index materials with good optical quality and negligible scattering. Thus, various innovative applications have been developed and thin Nb_2O_5 films have found applications in photonics for improving the optical performance of different devices such as optical filters [4], waveguide-based optical circuits [5], and transparent conductive electrodes [6]. A number of novel applications of Nb_2O_5 films rely on the ability to deposit high quality films using relatively simple and inexpensive techniques such as sol-gel and spin or dip coating. The sol-gel method attracts considerable scientific attention because of its versatility, low cost, and low temperature processing [7, 8]. Besides, it allows control of the microstructure of the coating and produces durable and chemically stable films. Moreover, the versatility of the sol-gel process to prepare porous film has an additional advantage to be exploited.

Mesoporous materials (pore diameter in the range of 2–50 nm) have attracted the scientific interest due to their remarkable properties and potential applications in many advanced areas such as drug delivery systems, sensors, catalysis, photovoltaic cells, and fuel cells [9]. One attractive application of the mesoporous films can be realized when they are incorporated in one-dimensional stacks (Bragg stacks) as high refractive index building blocks [10, 11]. In this case, an optical sensing could be realized on the basis of refractive index change due to the condensation of vapors in the pores [12–14].

Among several methods of porous films fabrication, the evaporation-induced self-assembly (EISA) process is the most advantageous because it offers good reproducibility and the reactions are finely controlled without any special techniques simply by changing sizes of the used templates and mole ratios of template to inorganic species [15–17]. Block copolymers are very attractive materials as soft-templating agents because they tend to self-assemble into micelles whose

Table 1: Refractive index (n), extinction coefficient (k), thickness (d), volume fractions of air (f_{air}) and acetone (f_{Ac}) in %, absolute reflectance change ΔR_{Ac}, and refractive index change Δn_{Ac} after exposure to acetone vapors as a function of Pluronic PE6100/$NbCl_5$ ratio.

Sample name	PE6100/$NbCl_5$	n(600 nm)	k (600 nm)	d (nm)	f_{air} (%)	ΔR_{Ac} (%)	Δn_{Ac}	f_{Ac} (%)
S1	0 : 1	2.198	$2.6 \cdot 10^{-2}$	44	0	0	0	0
S2	0.07 : 1	1.615	$2.4 \cdot 10^{-2}$	99	46	0.6	0.014	4.3
S3	0.14 : 1	1.668	$2 \cdot 10^{-2}$	94	41	0.5	0.011	4.2
S4	0.23 : 1	1.507	$1.8 \cdot 10^{-2}$	125	54	1.1	0.028	5.3
S5	0.46 : 1	1.513	$1.8 \cdot 10^{-2}$	124	54	0.88	0.023	5.3

morphology and size depend on block composition and solution parameters [18, 19].

Recently, we have shown that it is possible to control and optimize the optical and sensing properties of mesoporous Nb_2O_5 by changing the porosity degree and free volume fraction inside the films through varying the molar ratio of organic template (PE6800, BASF) and $NbCl_5$ used for preparing the Nb sol [20]. An improvement of sensing properties of mesoporous films is demonstrated as compared to the dense films (films prepared without template). However, despite the high volume fraction of free space inside the films (around 50%), only small amount of acetone is adsorbed (1.5%). Bad interconnectivity of the pores and their encapsulation inside the film are discussed as probable reasons for the weak response. In order to improve the sensing properties of thin Nb_2O_5 films, we intend to use Pluronic PE6100 as an organic template. As compared to PE6800, this template has four times lower molecular weight and 8 times lower percentage of polyethylene glycol (PEG) in the molecule. Moreover, in contrast to PE6800, PE6100 is insoluble in hydrochloric acid. Considering that Nb sol used for the preparation of the films consists of some amount of hydrochloric acid left as a side product from the synthesis, we expected PE6100 to lead to stronger porosity.

In the present paper, we study thin Nb_2O_5 films with tuned porosity prepared by the sol-gel and evaporation-induced methods using Pluronic PE6100 as an organic template. In order to tailor the porosity, different molar fractions of PE6100 with respect to $NbCl_5$ are used. Optical properties and thickness of the films are calculated from measured reflectance spectra through nonlinear curve fitting. Bruggeman effective medium approximation is applied for estimation of the overall porosity of the films and the amount of adsorbed acetone vapors in the pores. Reflectance spectra and room-temperature photoluminescence spectra collected prior to and after exposure to acetone are used for proving the sensing abilities of the films. The potential of using the studied mesoporous Nb_2O_5 films for chemooptical sensing is demonstrated and discussed.

2. Materials and Methods

Thin niobia (Nb_2O_5) films were prepared by spin-coating (3000 rpm, 30 s) of Nb sol and subsequent high temperature annealing at 320°C for 30 min at 5°C/min acceleration rate [8]. The Nb sol was synthesized by a sonocatalytic method using 0.400 g $NbCl_5$ (99%, Aldrich) as a precursor, 8.3 mL ethanol (98%, Sigma-Aldrich), and 0.17 mL distilled water [8].

The synthesis of mesoporous films was carried out through an evaporation-induced self-assembly method using organic template Pluronic PE6100 (BASF). PE6100 is a block copolymer in which the central polypropylene glycol group (PPG) is flanked by two polyethylene glycol groups (PEG). The molar mass of PPG and its percentage in the molecule are 1750 g/mol and 90%, respectively. The mass ratio of template to $NbCl_5$ for different samples is given in Table 1. After deposition, the template is eliminated by annealing at 320°C for 30 min at 5°C/min acceleration rate.

The surface morphology and structure of the films were studied by Transmission Electron Microscopy (TEM) and Selected Area Electron Diffraction (SAED) using HRTEM JEOL JEM 2100 (Japan) microscope.

The optical properties (refractive index (n) and extinction coefficient (k)) along with the thickness (d) of the films were determined from reflectance spectra of the films measured at normal light incidence by UV-VIS-NIR spectrophotometer Cary 05E (Varian, Australia) using nonlinear curve fitting method [8]. The experimental errors for n, k, and d are 0.005, 0.003, and 2 nm, respectively.

Photoluminescence spectra of the films were measured at excitation wavelength of 325 nm in the range of 340–640 nm using Fluorolog-3 spectrofluorometer (Horiba/Jobin-Yvon, France).

The vapor sensing measurements of the films were implemented in a Cary 05E spectrophotometer equipped with a homemade bubbler system for generation of vapors from liquids with controlled concentrations [11]. Reflectance spectra of the samples were measured before and after exposure to the vapors.

3. Results and Discussions

Figure 1 shows typical TEM images of the dense samples deposited without organic template (Figure 1(a)) and porous one obtained with addition of PE6100 in ratio of PE6100 : $NbCl_5$ = 0.07 : 1 (Figure 1(b)). The comparison of morphology shows that the template leads to the formation of pores in the mesosize range arranged nonperiodically. The SAED diffraction (shown as insets) had proven that all samples were amorphous. This result is consistent with our previous studies of sol-gel Nb_2O_5 films that revealed amorphous structure for film annealed at 320°C and crystalline one when films are annealed at 450°C [21].

Figure 2(a) presents reflectance spectra of the films in the spectral range from 320 to 900 nm. The comparison between dense film (s1) and porous ones (s2–s5) shows stepwise red

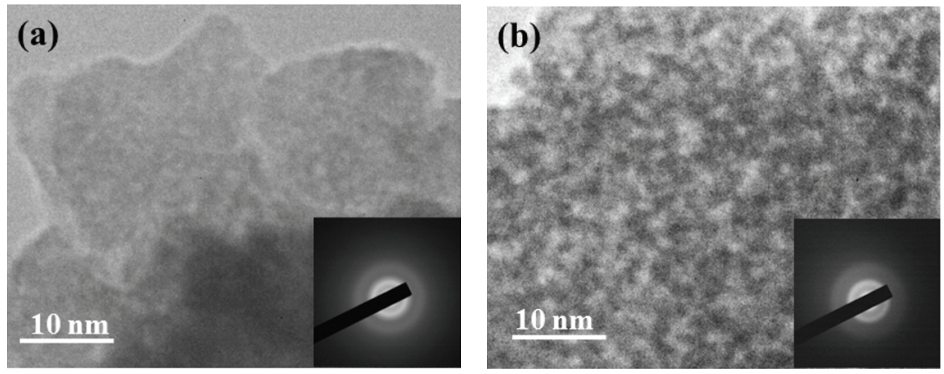

(a) (b)

FIGURE 1: TEM images of dense Nb_2O_5 film (a) and porous Nb_2O_5 film (b) prepared with the ratio of PE6100 : $NbCl_5$ equal to 0.07 : 1. SAED diffraction patterns are shown as insets.

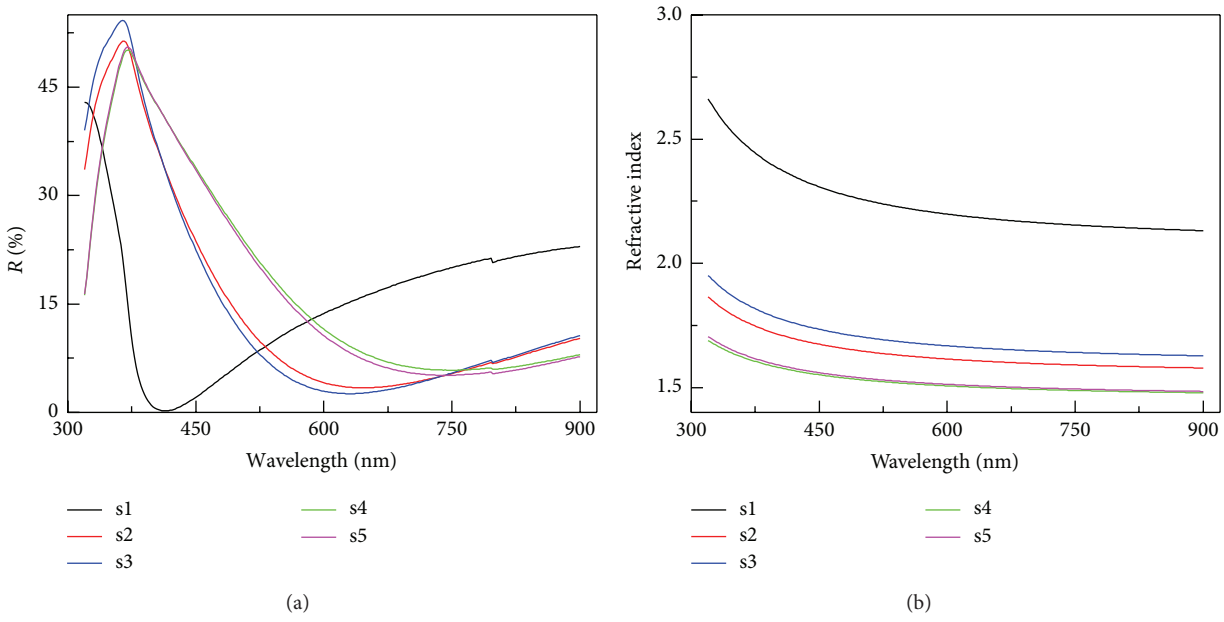

(a) (b)

FIGURE 2: Reflectance spectra (a) and refractive index dispersion curves (b) of the studied Nb_2O_5 films.

shift of the minima with increasing of the Pluronic concentration.

The measured spectra were further used for calculation of refractive index (n), extinction coefficient (k), and thickness (d) of the films. Figure 2(b) presents the dispersion curves of refractive index for the films with different amount of PE6100. All curves exhibit normal dispersion (n decreases with increasing of wavelength of light) that is expected for spectral region of slight absorption. With increasing the amount of PE from 0 to 0.07 (Table 1), a substantial decrease in n from 2.198 to 1.615 measured at 600 nm is observed. It is interesting to note that further increase of PE from 0.07 to 0.14 does not lead to additional significant change of n. The next decrease in n is observed for value of PE of 0.23: n changes from 1.668 to 1.507. No further reduction of n for s5 is noticed although PE increases twice as compared to s4.

The obtained dependencies for n are consistent with the data calculated for the films thickness. It is well known that refractive index is proportional to the density of films. It is seen from Table 1 that the biggest change of thickness (225%) is observed for the ratio 0.07 : 1. The increase in thickness is associated with reduction of density. Thus, the biggest decline in n is expected for the ratio 0.07 : 1. For further increase of the PE6100/$NbCl_5$ ratio, the change in d is less than 35% which means weaker reduction of density. This is the reason for big decrease of n for s2 (27%) and the smaller change for s4 and s5 (less than 10%).

The comparison between the results obtained for PE6100 and our previous results concerning porous films deposited with PE 6800 as a template [20] shows different behavior of R, n, and d when different templates are used. In the case of PE 6800, the refractive index and thickness

gradually change with Pluronic concentration. In contrast, PE 6100 results in a stepwise decrease in n and increase in d.

In order to estimate and compare the degree of porosity of the studied films, we calculated the free volume fractions in the films using Bruggeman effective medium approximation (BEMA). More details could be found elsewhere [20]. Briefly, the idea is to regard the porous film as an effective medium consisting of dense Nb_2O_5 and voids filled with air. The effective dielectric constant ε_e depends on the dielectric constants of the phases presented and their volume fractions:

$$f_d \frac{\varepsilon_d - \varepsilon_e}{\varepsilon_d + 2\varepsilon_e} + f_{\text{air}} \frac{\varepsilon_{\text{air}} - \varepsilon_e}{\varepsilon_{\text{air}} + 2\varepsilon_e} = 0, \qquad f_d + f_{\text{air}} = 1, \tag{1}$$

where ε_d and ε_{air} are the dielectric constants of dense Nb_2O_5 and air, respectively, and $f_d = V_d/V_{\text{tot}}$ and $f_{\text{air}} = V_{\text{air}}/V_{\text{tot}}$ are their volume fractions (with V_d and V_{air} being the volumes occupied by dense Nb_2O_5 and air, resp., $V_{\text{tot}} = V_d + V_{\text{air}}$ is the total volume of the film). For clarity, it is important to note that the two parameters ε and n are related as follows: $\varepsilon = n^2$. Thus, using the already determined values of refractive index n_d (sample s1) and n_e (samples s2, s3, s4, and s5) (ε_d and ε_e, resp.) (Figure 2(b)) and considering that $\varepsilon_{\text{air}} = 1$, the volume fraction of the voids f_{air} for each sample (s2, s3, s4, and s5) is calculated from (1) and presented in Table 1. It is seen from Table 1 that the free volume of the films varies from 40 to 55% with the biggest rise from 0 to 46% for the ratio of 0.07 (sample s2). Considering the significant increase of thickness (more than 200%) for s2, this result is not surprising.

The comparison between the porosity values for mesoporous Nb_2O_5 films obtained with different types of templates shows that in the case of PE6100 a significant amount of free volume is achieved for smaller ratios of PE6100 : $NbCl_5$. For example, for the lowest ratio studied (0.07 : 1), the free volumes in the samples are 46% and 22% when using PE6100 and PE6800, respectively. Thus, we concluded that more PPG in polymer molecule favors the generation of stronger porosity as compared to the case when PEG is prevailing.

It is seen from Table 1 that extinction coefficient decreases slightly with Pluronic addition. Considering that the amount of free volume increases with the amount of template added, it may be expected that for porous films the volume ratio of absorbing phase decreases, thus resulting in slightly smaller effective absorption.

The next step of our investigation concerns sensing properties of the samples. Purposely, the reflectance spectra of the samples are measured prior to and after exposure to acetone vapors at relative pressure $p/p_0 = 1$ (p_0 is the pressure of saturated vapors at zero degrees) generated from liquid using homemade bubbler system [11]. In order to make a comparison between samples, the exposure time is kept constant for all samples. The particular length of exposure is chosen to be 300 s. The values of reflectance changes $\Delta R_{\text{Ac}} = \text{abs}(R_{\text{Ac}} - R_{\text{Air}})$ (with R_{Air} and R_{Ac} being reflectance spectra before and after acetone exposure, resp., and "abs" denoting absolute value) are presented in Table 1 and Figure 3(a) with the respective errors. No change of R is observed for dense Nb_2O_5. For porous films, a stepwise increase of ΔR_{Ac} with Pluronic concentration is obtained: ΔR_{Ac} changes from 0 to 0.6% for samples s2 and s3 and to 1.1% for s5 and s6. The reason for the change in reflectance is acetone vapor condensation in the pores and replacement of the air inside with acetone with higher refractive index. As a result, the effective refractive index of the films increases leading to subsequent change in R (the sign of the change depends on the optical thickness/wavelength ratio).

From the viewpoint of comparative investigation, it is more convenient to calculate the absolute change of refractive index Δn_{Ac} using the already measured ΔR_{Ac}. Considering that R is a function of n, k, and d and assuming negligible changes in k and d due to acetone vapor exposure, we determine Δn_{Ac} from the following:

$$\Delta R_{\text{Ac}} = \frac{\partial R_{\text{Ac}}}{\partial n} \Delta n_{\text{Ac}}, \tag{2}$$

where $\partial R_{\text{Ac}}/\partial n$ and Δn_{Ac} are the partial derivatives of R_{Ac} with respect to n and the absolute change in n, respectively. The partial derivatives of R_{Ac} with respect to n are calculated numerically using

$$\frac{\partial R_{\text{Ac}}}{\partial n} = \frac{|R_1 - R_2|}{2\delta}, \tag{3}$$

where R_1 and R_2 are reflectance values calculated for two different values of refractive index ($n_{(a)} + \delta$) and ($n_{(a)} - \delta$), where δ ($= 10^{-9}$) is very small deviation from $n_{(a)}$ ($n_{(a)}$ is the refractive index of the film after exposure to acetone).

Figure 3(b) presents the calculated values of Δn_{Ac} in both cases of using PE6100 and PE6800 as templates. Similar to the previous dependencies, a stepwise change of Δn_{Ac} is observed when PE6100 ratio increases gradually from 0.07 to 0.46: Δn_{Ac} changes from 0 to 0.014 for s2 and s3 and to 0.028 for s4 and s5. The comparison with our previous results obtained with PE6800 (shown in Figure 3(b) as dark grey column bars) demonstrates that in the case of PE6100 the changes of n are stronger: Δn_{Ac} changes approximately four times more when using PE6100 as a template except for the molar ratio 0.14 where the changes are similar. We should note here that similar comparison between the values of ΔR_{Ac} obtained using different Pluronic types as templates is not correct if the thickness values of the films with the same concentration are different because reflectance depends on the film thickness as well in contrast to refractive index that is independent of d.

The values on Figure 3 are mean values of four measurements conducted on two samples for each molar ratio at two different points. The deviations from the mean value for each PE : $NbCl_5$ ratio are presented as error bars in Figure 3.

After acetone adsorption, the exposed films consist of three phases: dense Nb_2O_5, acetone, and air within the pores with respective dielectric functions ε_d, ε_{Ac}, and ε_{air} and

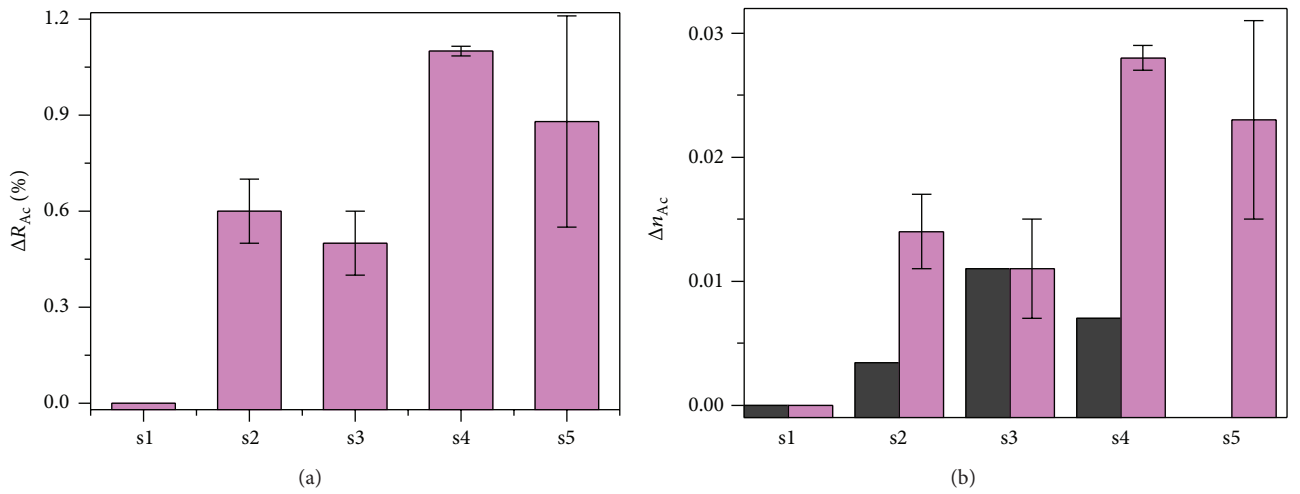

FIGURE 3: (a) Reflectance change ΔR_{Ac} in % and (b) refractive index change Δn_{Ac} after exposure to acetone vapors for samples with PE6100 (light magenta) and PE6800 (dark grey). Error bars are deviations from the mean value of four measurements conducted on two samples for each ratio at two different points.

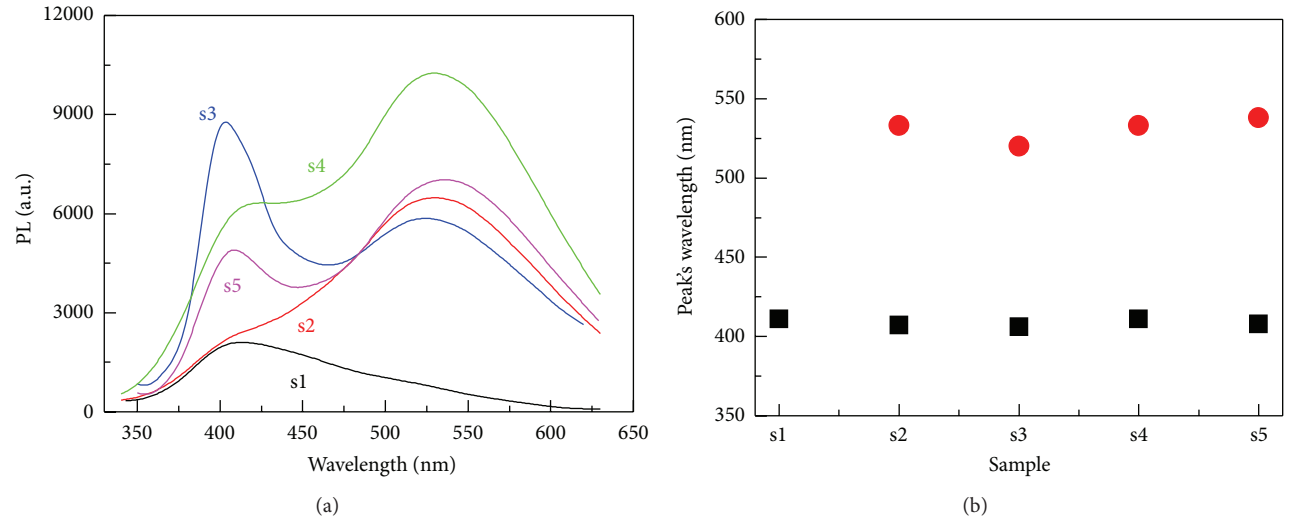

FIGURE 4: (a) Room-temperature photoluminescence spectra of the films measured at excitation wavelength of 325 nm and (b) wavelength position of PL peaks as a function of template fraction.

volume fractions $f_{d(a)}$, $f_{Ac(a)}$, and $f_{air(a)}$. Then, BEMA can be written in the following form:

$$f_{d(a)}\frac{\varepsilon_d - \varepsilon_{e(a)}}{\varepsilon_d + 2\varepsilon_{e(a)}} + f_{air(a)}\frac{\varepsilon_{air} - \varepsilon_{e(a)}}{\varepsilon_{air} + 2\varepsilon_{e(a)}} + f_{Ac}\frac{\varepsilon_{Ac} - \varepsilon_{e(a)}}{\varepsilon_{Ac} + 2\varepsilon_{e(a)}} = 0, \quad (4a)$$

$$f_{d(a)} + f_{air(a)} + f_{Ac} = 1, \quad (4b)$$

where $\varepsilon_{e(a)}$ is the dielectric function of the film after exposure to acetone vapors. The dielectric functions of air and dense Nb_2O_5, ε_{air}, and ε_d, respectively, are not affected by the acetone exposure and their values are the same as the values before acetone exposure.

In (4a), the dielectric functions of dense phase is already determined ($\varepsilon_d = n^2$, Table 1, sample s1), $\varepsilon_{Ac} = 1.85$ [20], $\varepsilon_{air} = 1$, and $\varepsilon_{e(a)} = (n_{(a)})^2 = (n + \Delta n_{Ac})^2$ (Table 1). Because the total volume of the sample does not change after exposure to acetone vapors, the volume fraction of the dense phase is the same ($f_{d(a)} = f_d = 1 - f_{air}$, where f_{air} is the volume fraction of air before acetone exposure, Table 1). Thus, all unknowns in (4a) are limited only to f_{Ac} and $f_{air(a)}$ that are easily determined with the help of (4b) (two equations for two unknowns). The calculated amount of adsorbed acetone as a function of added template is presented in Table 1. The comparison between f_{air} and f_{Ac} shows that for all samples with PE6100 the adsorbed amount of acetone is approximately 10% of the initial free space inside the films while for PE6800 maximum value of 10%

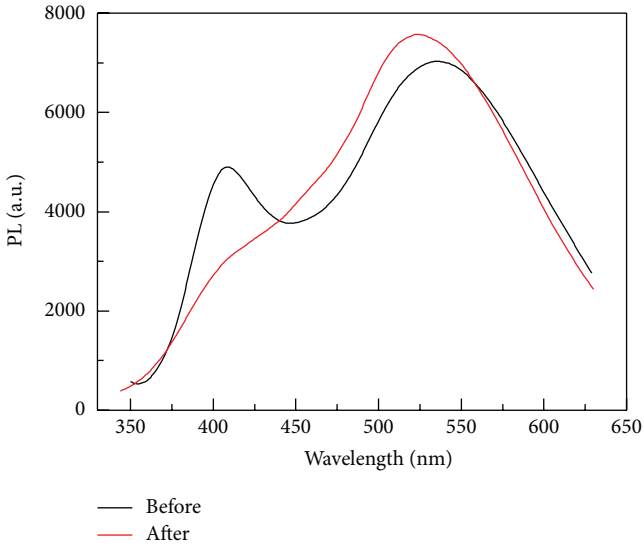

Figure 5: Room-temperature spectra of s5 before and after exposure to acetone.

is reached only for the sample with template ratio of 0.14 [20].

The final step of our investigation concerns the photoluminescence properties of the films and their change after exposure to liquid acetone. Figure 4(a) presents the photoluminescence (PL) spectra of the samples at room temperature excited at wavelength of 325 nm. A broad emission band is observed for dense Nb_2O_5 film centered at 411 nm that is consistent with reported data [22]. For porous films, an additional emission band appears at higher wavelength centered at approximately 530 nm and a great intensity growth is observed in comparison with the dense films.

PL emissions originate from the radiative recombination of photo-generated electrons and holes trapped in the band tails. These trapped electrons and holes are associated with the existence of nonbridging oxygen [23]. In wide-gap metal oxides like Nb_2O_5 PL emission is mainly related to the presence of defects in the solid, including the intrinsic defects due to impurities, vacancies, and interstitial atoms [24]. Usually the short wavelength emission is attributed to the near-band gap emission of Nb_2O_5 and the long wavelength PL is ascribed to the structure defects [25]. Thus, the low PL intensity can be correlated with both small concentration of nonbridging oxygen [23] in the dense film and low level of defects.

The additional long wavelength PL emission band could be ascribed to structure defects originated from the addition of pores in the dense Nb_2O_5 template. The PL intensity increases as the disorder in porous films increases. Simultaneously, there is no change of the positions of both PL emission bands (Figure 4(b)).

Figure 5 presents the PL spectra of sample s5 measured before and after exposure to liquid acetone. Sample s5 was chosen for the experiments because it contains the biggest amount of PE6100 and the defect levels for s5 are expected to be the highest. Moreover, both PL peaks for s5 are with similar intensities. This means that near-band gap emission and PL due to the structure defects contribute nearly the same to the overall PL spectra.

It is seen from Figure 5 that acetone has a distinct impact on the PL spectra: the short wavelength PL peak almost disappears and the long wavelength PL peak blue shifted with 13 nm. We may speculate that the polar nature and chemical structure of the acetone molecule have a "passivating" or "occupying" effect on the electronic states responsible for the short wavelength emission, thus suppressing the short wavelength PL peak. The weaker change of long wavelength peak suggests that the acetone affects the PL of the film through an electronic interaction, not through the generation of more defects and disorder.

4. Conclusions

Thin Nb_2O_5 films with tailored pore structure at the mesosize range are successfully deposited using combination of both sol-gel and evaporation-induced self-assembly methods. For the films preparation, mixtures of $NbCl_5$ and Pluronic PE6100 in different ratios are used. A growth in film thickness from 44 to 99 nm is observed when PE6100 : $NbCl_5$ ratio changes from 0 to 0.07. The thickness growth is associated with a substantial reduction of refractive index from 2.198 to 1.615. Simultaneously, a significant increase of the free volume fraction in film takes place. The comparison between the porosity values for mesoporous Nb_2O_5 films obtained with different types of templates shows that in the case of PE6100 a significant amount of free volume is achieved at smaller ratios of PE6100 : $NbCl_5$. For the lowest ratio studied (0.07 : 1), the free volumes are 46% and 22% when using PE6100 and PE6800, respectively. The conclusion made is that more PPG in polymer molecule favors the generation of stronger porosity as compared to the case when PEG is prevailing. Further increase of PE6100 : $NbCl_5$ ratio does not lead to remarkable change in n and d; n reaches value of 1.51 for the ratio of 0.23 and it is not changed further even when PE6100 : $NbCl_5$ ratio increases twice.

In addition, the potential application of films as sensitive elements of optical vapour sensors is demonstrated. An improvement of sensing properties of mesoporous films is realized as compared to both the dense films and the porous films deposited with the aid of PE6800 as a template. Refractive index changes stepwise when PE6100 concentration increases gradually and reaches value of 0.028 that is almost three times more as compared to the case of PE6800. Moreover, additional calculations show that for all films the adsorbed amount of acetone is approximately 10% of the free space inside the films while for PE6800 a maximum value of 10% is reached only for the film with template ratio of 0.14. For the rest of films with PE6800, only 3% of the free space is occupied with acetone after exposure to acetone vapors.

Room-temperature photoluminescence spectra measured at excitation wavelength of 325 nm showed single peak emission for dense film centered as 411 nm and an additional peak at 530 nm for porous films. The induced disorder and defects due to a presence of pores are the most probable

reason for increased PL for porous films as compared to dense one. Furthermore, a significant change of room-temperature photoluminescence spectra of porous films was observed when films are exposed to a drop of liquid acetone. The short wavelength PL peak almost disappears and the long wavelength PL peak blue shifted with 13 nm. On the basis of the observed significant change in the short wavelength peak and weaker change of the long wavelength PL peak, an assumption was made that the acetone affects the PL of the film through an electronic interaction, not through the generation of more defects and disorder.

Conflict of Interests

The authors declare that there is no conflict of interests regarding the publication of this paper.

Acknowledgments

The financial support from the project BG16 1P0003-1.2.04-0034-C0001 under Operational Programme "Development of the Competitiveness of the Bulgarian Economy" is highly appreciated. Tsvetanka Babeva would like to thank BASF (Bulgarian office) for supplying the polymers. The reviewer's help for interpretation of PL spectra after acetone exposure is highly appreciated.

References

[1] M. A. Aegerter, "Sol-gel chromogenic materials and devices," in *Optical and Electronic Phenomena in Sol-Gel Glasses and Modern Application*, C. K. Jorgensen and R. Reisfeld, Eds., vol. 85 of *Structure and Bonding*, pp. 149–194, Springer, Berlin, Germany, 1996.

[2] J. Gandhi, R. Dangi, and S. Bhardwaj, "Nb_2O_5 used as photocatalyst for degradation of methylene blue using solar energy," *Rasayan Journal of Chemistry*, vol. 1, no. 3, pp. 567–571, 2008.

[3] S. H. Mujawar, A. I. Inamdar, S. B. Patil, and P. S. Patil, "Electrochromic properties of spray-deposited niobium oxide thin films," *Solid State Ionics*, vol. 177, no. 37-38, pp. 3333–3338, 2006.

[4] C.-C. Lee, C.-L. Tien, and J.-C. Hsu, "Internal stress and optical properties of Nb_2O_5 thin films deposited by ion-beam sputtering," *Applied Optics*, vol. 41, no. 10, pp. 2043–2047, 2002.

[5] K. Mizuuchi, H. Ohta, K. Yamamoto, and M. Kato, "Second-harmonic generation with a high-index-clad waveguide," *Optics Letters*, vol. 22, no. 16, pp. 1217–1219, 1997.

[6] A. Dhar and T. L. Alford, "Optimization of Nb_2O_5/Ag/Nb_2O_5 multilayers as transparent composite electrode on flexible substrate with high figure of merit," *Journal of Applied Physics*, vol. 112, no. 10, Article ID 103113, 2012.

[7] M. A. Aegerter, "Sol-gel niobium pentoxide: a promising material for electrochromic coatings, batteries, nanocrystalline solar cells and catalysis," *Solar Energy Materials & Solar Cells*, vol. 68, no. 3-4, pp. 401–422, 2001.

[8] K. Lazarova, M. Vasileva, G. Marinov, and T. Babeva, "Optical characterization of sol-gel derived Nb_2O_5 thin films," *Optics and Laser Technology*, vol. 58, pp. 114–118, 2014.

[9] Y.-P. Zhu, T.-Z. Ren, and Z.-Y. Yuan, "Mesoporous non-siliceous inorganic-organic hybrids: a promising platform for designing multifunctional materials," *New Journal of Chemistry*, vol. 38, no. 5, pp. 1905–1922, 2014.

[10] T. Babeva, H. Awala, M. Vasileva et al., "Zeolite films as building blocks for antireflective coatings and vapor responsive Bragg stacks," *Dalton Transactions*, vol. 43, no. 23, pp. 8868–8876, 2014.

[11] K. Lazarova, H. Awala, S. Thomas, M. Vasileva, S. Mintova, and T. Babeva, "Vapor responsive one-dimensional photonic crystals from zeolite nanoparticles and metal oxide films for optical sensing," *Sensors*, vol. 14, no. 7, pp. 12207–12218, 2014.

[12] G. J. A. A. Soler-Illia, P. C. Angelomé, M. C. Fuertes et al., "Mesoporous hybrid and nanocomposite thin films. A sol-gel toolbox to create nanoconfined systems with localized chemical properties," *Journal of Sol-Gel Science and Technology*, vol. 57, no. 3, pp. 299–312, 2011.

[13] M. N. Ghazzal, O. Deparis, A. Errachid et al., "Porosity control and surface sensitivity of titania/silica mesoporous multilayer coatings: applications to optical Bragg resonance tuning and molecular sensing," *Journal of Materials Chemistry*, vol. 22, no. 48, pp. 25302–25310, 2012.

[14] M. C. Fuertes, F. J. López-Alcaraz, M. C. Marchi et al., "Photonic crystals from ordered mesoporous thin-film functional building blocks," *Advanced Functional Materials*, vol. 17, no. 8, pp. 1247–1254, 2007.

[15] Y. Ren, Z. Ma, and P. G. Bruce, "Ordered mesoporous metal oxides: synthesis and applications," *Chemical Society Reviews*, vol. 41, no. 14, pp. 4909–4927, 2012.

[16] C. García-Sancho, J. M. Rubio-Caballero, J. M. Mérida-Robles, R. Moreno-Tost, J. Santamaría-González, and P. Maireles-Torres, "Mesoporous Nb_2O_5 as solid acid catalyst for dehydration of D-xylose into furfural," *Catalysis Today*, vol. 234, pp. 119–124, 2014.

[17] F. Hashemzadeh, R. Rahimi, and A. Ghaffarinejad, "Mesoporous nanostructures of Nb_2O_5 obtained by an EISA route for the treatment of malachite green dye-contaminated aqueous solution under UV and visible light irradiation," *Ceramics International*, vol. 40, no. 7, pp. 9817–9829, 2014.

[18] D. Gu and F. Schüth, "Synthesis of non-siliceous mesoporous oxides," *Chemical Society Reviews*, vol. 43, no. 1, pp. 313–344, 2014.

[19] R. Nisticò, D. Scalarone, and G. Magnacca, "Preparation and physico-chemical characterization of large-mesopore silica thin films templated by block copolymers for membrane technology," *Microporous and Mesoporous Materials*, vol. 190, pp. 208–214, 2014.

[20] K. Lazarova, B. Georgieva, M. Spasova, and T. Babeva, "Preparation and characterization of mesoporous Nb_2O_5 films for sensing applications," *Journal of Physics: Conference Series*, vol. 558, Article ID 012042, 2014.

[21] K. Lazarova, M. Vasileva, G. Marinov, and T. Babeva, "Sol-gel derived Nb_2O_5 thin films for photonic applications," *Bulgarian Chemical Communications*, vol. 45, pp. 23–27, 2013.

[22] J. Yan, G. Wu, N. Guan, and L. Li, "Nb_2O_5/TiO_2 heterojunctions: synthesis strategy and photocatalytic activity," *Applied Catalysis B: Environmental*, vol. 152-153, no. 1, pp. 280–288, 2014.

[23] E. R. Leite, F. M. Pontes, E. J. H. Lee et al., "A novel approach for the development of photoluminescent material," *Applied Physics A: Materials Science and Processing*, vol. 74, no. 4, pp. 529–532, 2002.

[24] H. Zhu, Z. Zheng, X. Gao et al., "Structural evolution in a hydrothermal reaction between Nb_2O_5 and NaOH solution: from Nb_2O_5 grains to microporous $Na_2Nb_2O_6 \cdot {}^2/_3H_2O$ fibers and $NaNbO_3$ cubes," *Journal of the American Chemical Society*, vol. 128, no. 7, pp. 2373–2384, 2006.

[25] Y. Zhou, Z. Qiu, M. Lü, A. Zhang, and Q. Ma, "Preparation and spectroscopic properties of Nb_2O_5 nanorods," *Journal of Luminescence*, vol. 128, no. 8, pp. 1369–1372, 2008.